Tenth-order high-temperature expansion for the susceptibility and the specific heat of spin-s Heisenberg models with arbitrary exchange patterns: Application to pyrochlore and kagome magnets

Andre Lohmann,[1] Heinz-Jürgen Schmidt,[2] and Johannes Richter[1,*]

[1]*Institut für Theoretische Physik, Otto-von-Guericke-Universität Magdeburg, PF 4120, D-39016 Magdeburg, Germany*

[2]*Universität Osnabrück, Fachbereich Physik, Barbarastraße 7, D-49069 Osnabrück, Germany*

(Received 3 September 2013; revised manuscript received 12 December 2013; published 15 January 2014)

We present the high-temperature expansion (HTE) up to tenth order of the specific heat C and the uniform susceptibility χ for Heisenberg models with arbitrary exchange patterns and arbitrary spin quantum number s. We encode the algorithm in a C++ program provided in the Supplemental Material [http://link.aps.org/supplemental/10.1103/PhysRevB.89.014415] which allows to explicitly get the HTE series for concrete Heisenberg models. We apply our algorithm to pyrochlore ferromagnets and kagome antiferromagnets using several Padé approximants for the HTE series. For the pyrochlore ferromagnet, we use the HTE data for χ to estimate the Curie temperature T_c as a function of the spin quantum number s. We find that T_c is smaller than that for the simple-cubic lattice, although both lattices have the same coordination number. For the kagome antiferromagnet, the influence of the spin quantum number s on the susceptibility as a function of renormalized temperature $T/s(s+1)$ is rather weak for temperatures down to $T/s(s+1) \sim 0.3$. On the other hand, the specific heat as a function of $T/s(s+1)$ noticeably depends on s. The characteristic maximum in $C(T)$ is monotonously shifted to lower values of $T/s(s+1)$ when increasing s.

DOI: 10.1103/PhysRevB.89.014415 PACS number(s): 75.10.Jm, 75.40.Gb

I. INTRODUCTION

Magnetic systems described by the Heisenberg Hamiltonian,

$$H = \sum_{\mu<\nu} J_{\mu\nu} \mathbf{s}_\mu \cdot \mathbf{s}_\nu \tag{1}$$

are an active field of theoretical and experimental research.[1] The accurate description of these quantum many-body systems is the basic aim of theoretical investigations. The comparison with experimental studies typically requires the calculation of the temperature dependence of physical properties, such as the susceptibility χ and the specific heat C. For unfrustrated spin systems, the quantum Monte Carlo (MC) technique is a suitable tool to provide precise data, but it is not applicable due to the sign problem for frustrated quantum spin models.[2] Hence, reliable results for strongly frustrated quantum spin models are notoriously rare. Since there is very active research in the field of frustrated quantum magnetism, see, e.g., Refs. 1, 3, and 4, and references therein, theoretical methods to calculate thermodynamic quantities in the presence of frustration are highly desirable. One of the most interesting systems is the kagome Heisenberg antiferromagnet, which we will consider in Sec. III B. This highly frustrated magnetic system has extensively been investigated theoretically for spin quantum number $s = 1/2$, see, e.g., Refs. 5–17 and in the classical limit $s \to \infty$, see, e.g., Refs. 18–22. On the experimental side, several kagome compounds have $s > 1/2$, however, the theoretical study of quantum models with $s > 1/2$ lags behind.

A universal straightforward approach to calculate thermodynamic quantities for unfrustrated as well as frustrated magnetic systems is the high-temperature expansion (HTE). For Heisenberg models, this method was introduced in an early paper by Opechowski,[23] which is based on a method of approximate evaluation of the partition function. In the 1950s and 1960s, the method was further developed and was widely applied to various Heisenberg systems, see, e.g., Refs. 24–28.

The HTE method is now well established, and its application to magnetic systems is a basic tool in theoretical physics, see Refs. 29 and 30, and references therein. Now, for the Heisenberg model with nearest-neighbor (NN) interaction on standard lattices, typically, the HTE is known up to high orders, see, for example, Refs. 31, 32, and 33 where the HTE up to 14th order for the triangular lattice and up to 16th order for the kagome and hyperkagome lattices were published. On the other hand, often, magnetic compounds and corresponding spin models are of interest where two, three, or even more exchange constants are relevant. Typical examples are magnetic systems with nearest-neighbor, next-nearest-neighbor, and third-nearest-neighbor couplings, see, e.g., Ref. 34. Moreover, in most of the quasi-low-dimensional magnetic compounds, interchain or interlayer couplings play a role, see, e.g., Ref. 35. Note further that available high-order HTEs often are restricted to spin quantum number $s = 1/2$, see, e.g., Refs. 31, 32, 33, 36, and 37 as examples. As a rule, for such more complex exchange geometries and/or higher spin quantum numbers $s > 1/2$, relevant for the interpretation of experimental data, the HTE is not available in higher orders. An earlier attempt to bridge this gap was published in Ref. 38 where general analytical HTE expressions were given for arbitrary s and arbitrary Heisenberg exchange couplings up to order three. Very recently, the present authors have published a significant extension of this paper using computer algebraic tools.[39] In that paper, the HTE algorithm for general spin-s Heisenberg models up to eighth order was presented. This algorithm was encoded as a C++ program. The download[40] and use are free. Thus, this algorithm provides a flexible tool for the community to compute the HTE for the susceptibility and the specific heat, which can be used to analyze the

thermodynamics of spin models, to check approximations, and, last but not least, to compare experimental data with model predictions.

In our previous paper,[39] we considered several models. Our results demonstrated that the eighth-order HTE with a subsequent Padé approximation is able to correctly describe the maximum of the susceptibility of a square lattice $s = 1/2$ Heisenberg antiferromagnet, can yield better results for spin systems in dimension $d > 1$ than full exact diagonalization, and gives good agreement with Monte Carlo data for the classical pyrochlore antiferromagnet down to temperatures of about 40% of the exchange coupling.

The aim of the present paper is twofold. On one hand, we will extend our earlier approach[39] up to tenth order for general Heisenberg Hamiltonians (Sec. II). Again, we provide this new extended tool as a freely accessible C++ program, see Supplemental Material[41] and Ref. 42, where, except for the code, a manual on how to use the code can also can be found. On the other hand, results for the susceptibility and the specific heat for the spin-s Heisenberg model on the pyrochlore and the kagome lattices are provided (Sec. III), which we will use to discuss the influence of the spin quantum number on the thermodynamics of these models. In Appendixes A and B, we explicitly present the HTE series for the pyrochlore and the kagome spin-s Heisenberg magnets. In the Supplemental Material,[41] we present the detailed results for the tenth-order HTE of specific heat and susceptibility and the auxiliary quantities to be introduced in Sec. II.

II. BRIEF EXPLANATION OF THE METHOD

We consider the HTE expansion of extensive quantities f, e.g., susceptibility χ or specific heat C, of the form

$$f^{\Sigma}(\beta) = \sum_{n=0}^{\infty} c_n^{\Sigma,f} \beta^n. \tag{2}$$

Here β is the inverse dimensionless temperature $\beta = \frac{J}{k_B T}$, where J is a typical exchange energy, and the index Σ indicates the dependence on the spin system Σ, which is given by the Hamiltonian (1) and the value of the spin quantum number s. A further dependence on the magnetic field is possible but is neglected in this paper. As mentioned in the Introduction, we do not consider special systems Σ but rather look for a general HTE expansion valid for arbitrary Heisenberg systems.

Interestingly, the coefficients $c_n^{\Sigma,f}$ in (2) can be written in the form of scalar products between two vectors Q and p such that the first vector Q only depends on the spin system Σ but not on s, and the second one p only depends on the considered quantity f and the spin quantum number s. The index set of vectors p and Q can be identified with finite sets G_n^f of multigraphs, see Ref. 39 for the details. Thus, the scalar product of Q and p is a sum over multigraphs $\mathcal{G} \in G_n^f$,

$$c_n^{\Sigma,f} = \sum_{\mathcal{G}\in G_n^f} Q^{\Sigma}(\mathcal{G}) p^f(\mathcal{G}). \tag{3}$$

To give an elementary example, consider $f = \chi$, the zero-field uniform susceptibility. Simplifying the notation a bit, we may write

$$\chi(\beta) = Q(\mathcal{G}_0)p_0\beta + Q(\mathcal{G}_1)p_1\beta^2 + [Q(\mathcal{G}_2)p_2 + Q(\mathcal{G}_3)p_3]\beta^3 + O(\beta^4). \tag{4}$$

Here

$$p_0 = \tfrac{1}{3}r, \qquad r \equiv s(s+1), \tag{5}$$

$$p_1 = -\tfrac{2}{9}r^2, \qquad p_2 = -\tfrac{1}{18}r^2, \qquad p_3 = \tfrac{2}{27}r^3, \tag{6}$$

$\mathcal{G}_0 =$, $\mathcal{G}_1 =$, $\mathcal{G}_2 =$, $\mathcal{G}_3 =$, (7)

$$Q(\mathcal{G}_0) = N \quad \text{(number of spins)}, \tag{8}$$

$$Q(\mathcal{G}_1) = \sum_{\mu<\nu} J_{\mu\nu}, \qquad Q(\mathcal{G}_2) = \sum_{\mu<\nu} J_{\mu\nu}^2, \tag{9}$$

$$Q(\mathcal{G}_3) = \sum_{\lambda<\mu<\nu} J_{\lambda\mu} J_{\mu\nu}. \tag{10}$$

In this example, the $p^f(\mathcal{G})$'s are polynomials in the variable $r \equiv s(s+1)$ of the form $p^f(\mathcal{G}) = \sum_{\nu=0}^{n} a_\nu r^\nu$, where n is the order of HTE in (3). This holds, in general. Also, generally, the $Q^{\Sigma}(\mathcal{G})$'s are polynomials in the coupling constants $J_{\mu\nu}$ that can be calculated by considering the various ways of embedding graph $\mathcal{G}$ into the spin system. For example, each mapping of the three-chain onto three spins with numbers $\lambda < \mu < \nu$ gives rise to a term $J_{\lambda\mu}J_{\mu\nu}$ in $Q^{\Sigma}(\mathcal{G})$. The condition $\lambda < \mu < \nu$ guarantees that different embeddings resulting from symmetries of $\mathcal{G}$ are counted only once. Also this is typical for the general situation.

If the spin system is an infinite lattice, the $Q^{\Sigma}(\mathcal{G})$'s have to be redefined by first considering finite realizations of Σ and then dividing by the number of spins N and considering the thermodynamic limit $N \longrightarrow \infty$. If $\mathcal{G}$ is not connected, then $Q^{\Sigma}(\mathcal{G})$ would scale with N^c, where c is the number of connected components of $\mathcal{G}$. Hence, for the sake of consistency, the sets G_n^f must only consist of connected graphs. Keeping this in mind, the coefficients $c_n^{\Sigma,f}$ obtained represent rigorous results on infinite spin lattices that are notoriously rare.

For the determination of $Q^{\Sigma}(\mathcal{G})$, there exist effective computer programs. On the other hand, we have determined the universal polynomials $p^f(\mathcal{G})$ for $f = \chi, C$ and $\gamma(\mathcal{G}) \leqslant 10$, see Ref. 41. The method used has been explained to some detail in Ref. 39 and will only be sketched here. The crucial auxiliary data are the polynomials $p^{(t)}(\mathcal{G})(r)$ resulting from the moments of the Heisenberg Hamiltonian (1) via

$$\tilde{t}_n \equiv \operatorname{Tr} H^n = (2s+1)^n \sum_{\mathcal{G}\in G_n^{(t)}} Q^{\Sigma}(\mathcal{G}) p^{(t)}(\mathcal{G}). \tag{11}$$

In this case, the polynomials can be shown to be of the form $p^{(t)}(\mathcal{G}) = \sum_{\nu=g}^{\gamma} a_\nu r^\nu$, where $g = g(\mathcal{G})$ is the number of vertices of $\mathcal{G}$ and $\gamma = \gamma(\mathcal{G})$ is the number of edges. These polynomials have essentially been determined by numerically calculating $\operatorname{Tr} H^n$ and $Q^{\Sigma}(\mathcal{G})$ for a suitable number of randomly chosen spin systems and then solving the linear

system of equations (11) for $p^{(t)}(\mathcal{G})$. This has to be repeated for different values of $s = 1/2, 1, 3/2, \ldots$, in order to estimate the rational coefficients of the polynomials $p^{(t)}(\mathcal{G})(r)$, $r = s(s+1)$. Additionally, partial analytical results from Refs. 29 and 39 have been used, and various cross checks have been performed.

As described in Ref. 39, from $p^{(t)}(\mathcal{G})$, one deduces the "magnetic moments,"

$$\tilde{\mu}_n \equiv \mathrm{Tr}\left(S_3^2 H^n\right) = (2s+1)^n \sum_{\mathcal{G}\in G_n^{(m)}} Q^{\Sigma}(\mathcal{G}) p^{(m)}(\mathcal{G}), \quad (12)$$

and, from $\tilde{t}_n$ and $\tilde{\mu}_n$, the HTE series for $C(\beta)$ and $\chi(\beta)$. In this last step, products of $Q^{\Sigma}(\mathcal{G}_\mu)$ will occur as well as contributions from disconnected graphs. In order to obtain manifestly extensive quantities, these various nonextensive terms have to cancel by means of certain "product rules" of the form

$$Q^{\Sigma}(\mathcal{G}_\mu) Q^{\Sigma}(\mathcal{G}_\nu) = \sum_{\lambda} c^{\lambda}_{\mu\nu} Q^{\Sigma}(\mathcal{G}_\lambda). \quad (13)$$

All calculations described in this section involve a total number of 7355 graphs. Especially, those steps leading from the moments to the HTE series have been performed with the aid of the computer algebra system MATHEMATICA 8.0.

III. APPLICATIONS

The region of validity of the HTE can be extended by Padé approximants[43] (see also, Refs. 29 and 30). The Padé approximants are ratios of two polynomials $[m,n] = P_m(x)/R_n(x)$ of degrees m and n, and they provide an analytic continuation of a function $f(x)$ given by a power series. As a rule, approximants with $m \sim n$ provide the best results. Since we have a power series up to tenth order, here we use the corresponding [4,6], [5,5], and [6,4] Padé approximants. As in our previous paper,[39] we will present the temperature dependence of physical quantities using a renormalized temperature $T/s(s+1)$.

A. The pyrochlore Heisenberg ferromagnet

The pyrochlore antiferromagnet has attracted much attention over the past years as an example of a highly frustrated three-dimensional (3D) magnetic system, see, e.g. Refs. 44–46, and references therein. In our previous paper,[39] we have already presented the analytical expressions for χ and C up to order eight as well as the temperature dependence of the susceptibility for the pyrochlore Heisenberg antiferromagnet where very good agreement of the [4,4] Padé approximant with classical Monte Carlo results down to temperatures of about 40% of the exchange coupling was found. The new terms of HTE in orders nine and ten can be found in Appendix A.

Here we consider the ferromagnetic case. We consider only nearest-neighbor bonds and set $J_{\mu\nu} = J = -1$ for neighboring sites μ and ν. We want to demonstrate that the tenth-order HTE is an appropriate tool to determine the critical (Curie) temperature T_c for 3D ferromagnets. In Fig. 1, we show the Padé approximant [4,6] of the inverse susceptibility $1/\chi$. We see the typical behavior of a 3D ferromagnet. The extreme quantum case $s = 1/2$ is somewhat separated from the other curves, but

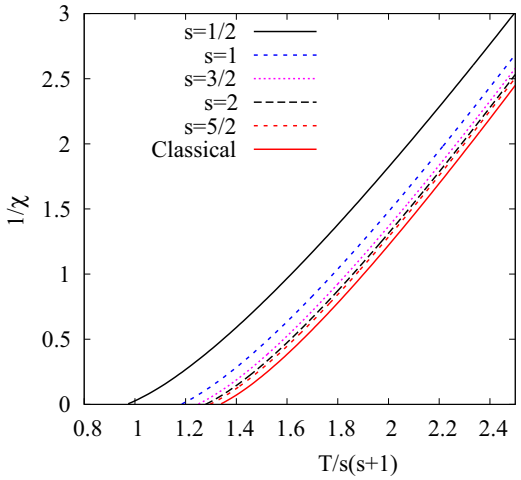

FIG. 1. (Color online) Padé approximant [4,6] of the inverse susceptibility $1/\chi$ of the pyrochlore Heisenberg ferromagnet for various spin quantum numbers s.

for $s > 1$, the curves are very close to each other. The zeros of the $1/\chi(T)$ curves can be understood as an estimate of the critical temperature. More sophisticated methods exploit the behavior of the expansion coefficients c_n, see Eq. (2), for the susceptibility to determine T_c, see, e.g., Refs. 24, 26, and 47. One variant is to analyze the quotient $q_n = c_n/c_{n-1}$. If the critical behavior of χ is given by $\chi(T) \propto (T - T_c)^{-\lambda}$, $T \to T_c + 0$, in the limit $n \to \infty$, this quotient depends linearly on $1/n$ according to $q_n = \frac{kT_c}{J} + (\lambda - 1)\frac{kT_c}{Jn}$. Hence, we get $\frac{kT_c}{J}$ by $\lim_{n\to\infty} q_n = \frac{kT_c}{J}$.

We performed a linear fit of our HTE data for q_n including data points for $n = 5, \ldots, 10$ to get an approximate value for T_c. Our results for T_c are shown in Fig. 2. For comparison, we also show T_c data for the simple-cubic ferromagnet where precise Monte Carlo data are available for $s = 1/2$ (Ref. 48) and for $s \to \infty$ (Ref. 49), which yield an impression of the accuracy of the HTE estimate of T_c. Except for the $(s = 1/2)$-pyrochlore case, the q_n data follow a straight line reasonably

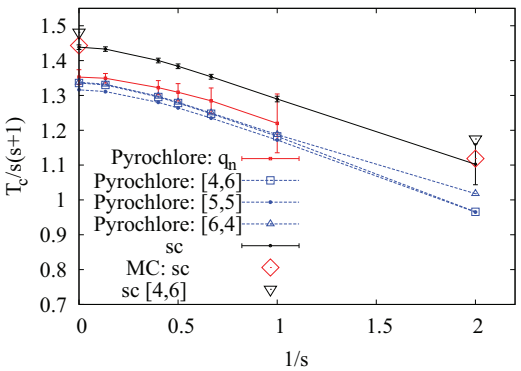

FIG. 2. (Color online) Curie temperature T_c in dependence on the inverse spin quantum number $1/s$ of the pyrochlore Heisenberg ferromagnet for $s = 1/2$, 1, 3/2, 2, 5/2, 15/2, and $s \to \infty$. For comparison, we also show the T_c values for the simple-cubic Heisenberg ferromagnet. The Monte Carlo data (MC) for $s = 1/2$ and $s \to \infty$ are taken from Refs. 48 and 49, respectively.

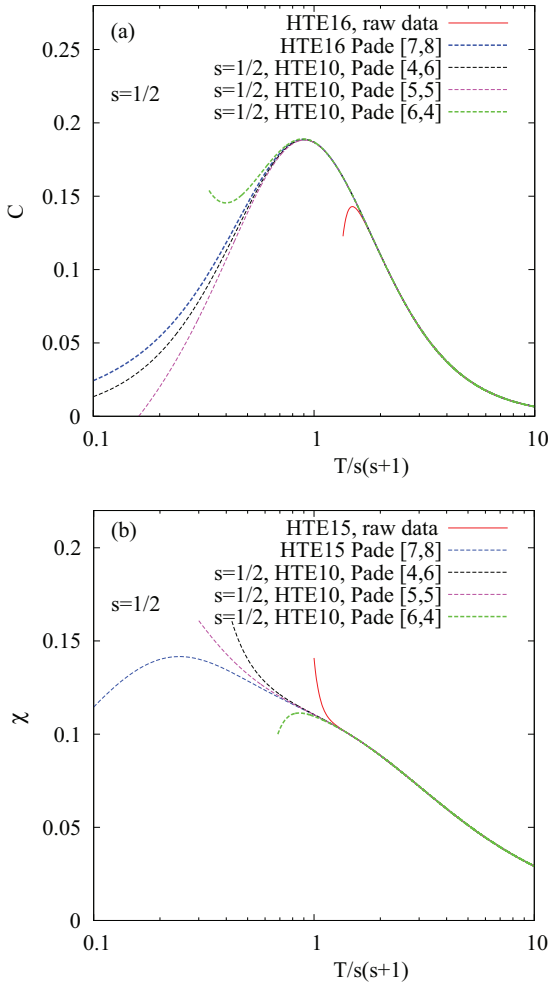

FIG. 3. (Color online) (a) Specific heat C and (b) susceptibility χ of the $s = 1/2$ kagome Heisenberg antiferromagnet. For comparison, we show the raw data of the 15th/16th-order HTEs and the corresponding Padé [7,8] approximant taken from Ref. 32.

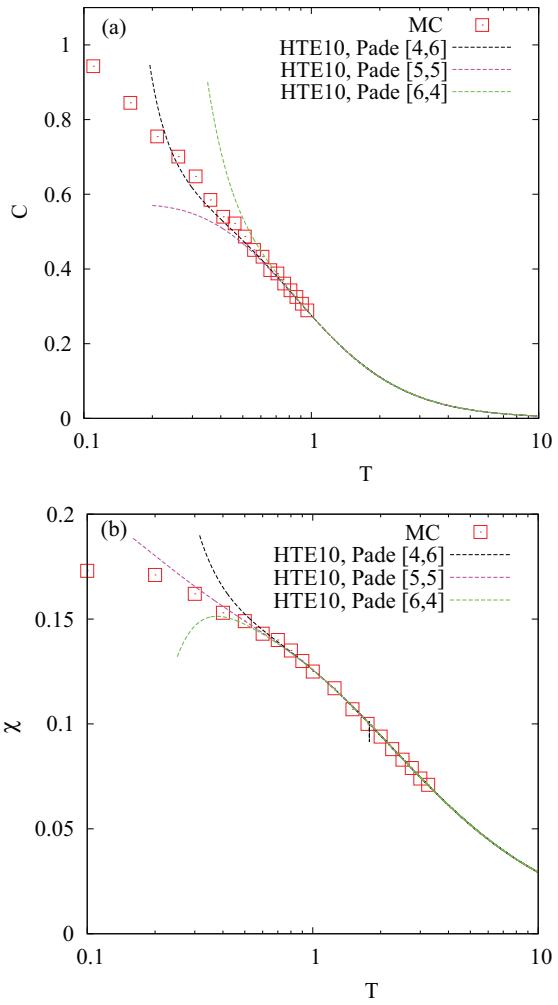

FIG. 4. (Color online) (a) Specific heat C and (b) susceptibility χ of the classical kagome Heisenberg antiferromagnet. For comparison, we show the Monte Carlo data (MC) taken from Ref. 20.

well (see also, the error bars in Fig. 2). For the ($s = 1/2$)-pyrochlore ferromagnet, the linear fit of the q_n data due to extremely large fluctuations in the data fails.[50] The comparison with the Monte Carlo data for the simple-cubic ferromagnet demonstrates that, indeed, the HTE series up to order ten for the susceptibility may yield accurate values for T_c. Already the poles in the Padé approximants provide reasonable results (we have about a 14% deviation from Monte Carlo data for $s = 1/2$ and about 9% for $s \to \infty$). The linear fit of q_n is even very close to the Monte Carlo results. Unfortunately, we did not find data for T_c of the pyrochlore ferromagnet in the literature to compare with our HTE data.

Comparing the pyrochlore and simple-cubic lattices, we find that T_c is significantly lower for the pyrochlore lattice. (Note that a simple molecular-field approximation would lead to identical values of T_c since both lattices have the same coordination number.) A similar finding was reported in Ref. 51 where the Curie temperatures of the stacked square and a stacked kagome ferromagnet were compared. In analogy to the discussion in Ref. 51, we may attribute the lower T_c values of the pyrochlore lattice to geometric frustration. For the ferromagnetic ground state, frustration is irrelevant, i.e., the ground-state energies are identical for the pyrochlore and simple-cubic ferromagnets. However, due to frustration, the upper bound of the eigenenergies (related to the absolute value of the ground-state energy of the corresponding antiferromagnet) is much lower for the pyrochlore ferromagnet than that for the simple-cubic lattice. Hence, one can expect that excited states with antiferromagnetic spin correlations have lower energy for the pyrochlore ferromagnet, resulting in a larger contribution to the partition function at a certain finite temperature T in comparison with the simple-cubic ferromagnet.

B. The kagome Heisenberg antiferromagnet

The two-dimensional kagome antiferromagnet is one of the most interesting and challenging spin models. There are numerous papers investigating the ground state of the $s = 1/2$ case, see, e.g., Refs. 5–17, 52, and 53, and references therein, but so far, no conclusive answer on the nature of the ground state and the existence of a spin gap has been found. The finite-temperature properties also are widely discussed

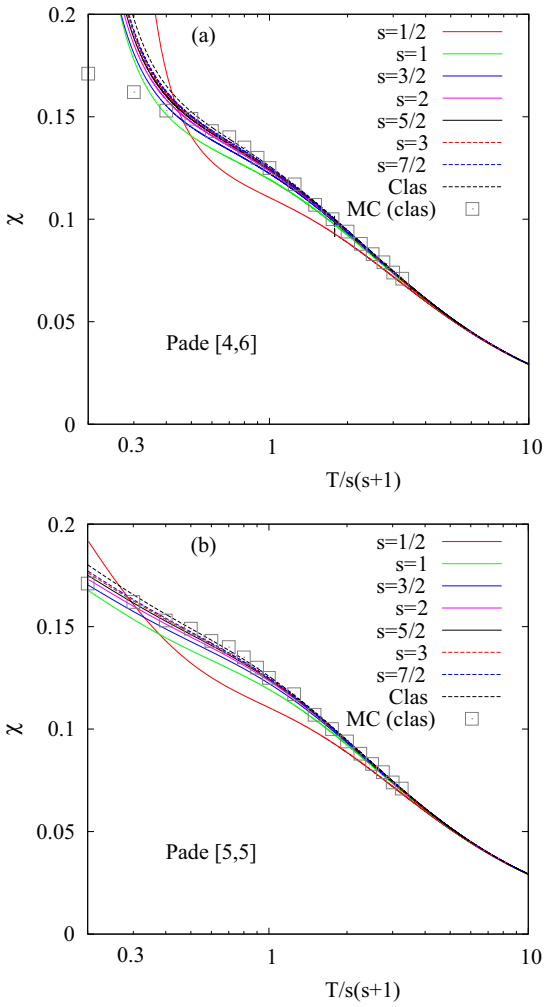

FIG. 5. (Color online) HTE data for the susceptibility χ of the spin-s kagome Heisenberg antiferromagnet, (a) Padé [4,6] and (b) Padé [5,5]. For comparison, we show the Monte Carlo data (MC) taken from Ref. 20.

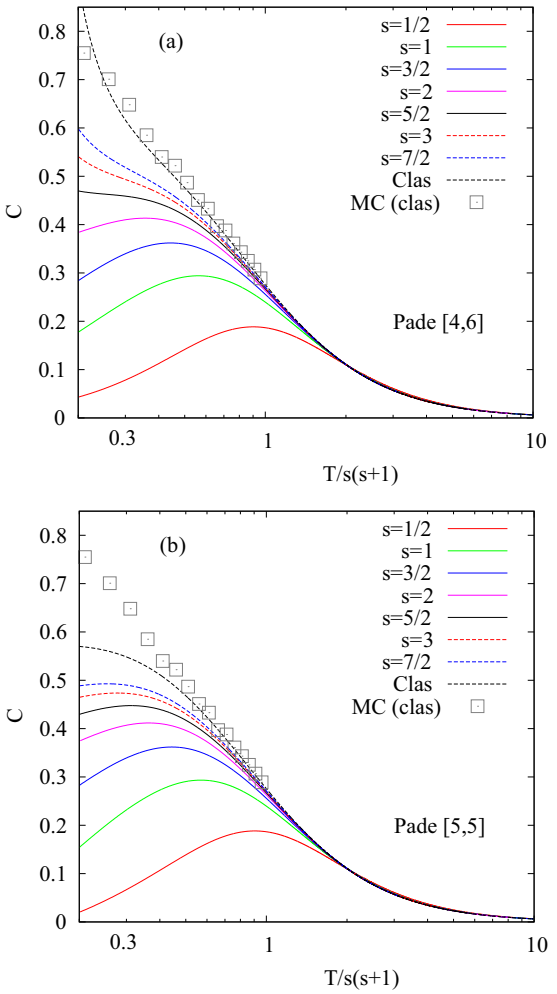

FIG. 6. (Color online) Specific heat C of the spin-s kagome Heisenberg antiferromagnet, (a) Padé [4,6] and (b) Padé [5,5]. For comparison, we show the Monte Carlo data (MC) taken from Ref. 20.

for the spin-1/2 model, including the analysis of the HTE series.[32,54–60] On the other hand, there are several kagome compounds with spin quantum number $s > 1/2$. We mention the jarosite compounds with $s = 5/2$ (see, e.g., Refs. 61 and 62), the magnetic compounds $KCr_3(OD)_6(SO_4)_2$ (Ref. 63) and $SrCr_{9p}Ga_{12-9p}O_{19}$ (Ref. 64) with $s = 3/2$, and the recently synthesized $BaNi3(OH)_2(VO4)_2$ (Ref. 65) compound with $s = 1$. For $s = 5/2$, one may expect that a classical Monte Carlo approach[18–22] might be reasonable, but for $s = 1$ and for $s = 3/2$, certainly quantum effects are important. However, we will see that at least for the specific heat, the classical Monte Carlo data significantly deviate from the data for $s = 5/2$, see below.

We present the HTE series for χ and C up to order ten and for arbitrary s in Appendix B. Remember that, in Ref. 32, the HTE series for $s = 1/2$ for χ (C) was given up to order 15 (16).[66] As a benchmark test, in Figs. 3 and 4, we first compare our HTE-Padé data with available data for the $s = 1/2$ model[32] and for the classical model.[20] This comparison leads to the conclusion that: (i) the [4,6] and [5,5] Padé approximants are favorable and that (ii) our HTE-Padé data are quite accurate down to temperatures $T/s(s+1) \sim 0.5$ ($T \sim 0.4$) for $s = 1/2$ (classical limit). In particular, the maximum in C, present for the $s = 1/2$ model at $T/s(s+1) \sim 0.9$, cf. Refs. 32 and 54–59, is correctly described by our Padé approximants. Note, however, that for $s = 1/2$, there are indications for a second low-temperature maximum in $C(T)$ below $T/s(s+1) = 0.1$, see Refs. 32, 55, 56, and 58, which is not covered by our HTE approach. Another characteristic feature is the shoulder present in $\chi(T)$ for $s = 1/2$ at about $T/s(s+1) = 1$, which also is well described by our Padé approximants.

In Figs. 5 and 6, we compare the $\chi(T)$ (Fig. 5) and $C(T)$ data (Fig. 6) for spin quantum numbers $s = 1/2, 1, \ldots, 7/2, \infty$. The susceptibility data clearly show that all curves for $s > 1/2$ form a narrow bundle in the temperature range accessible by our approach. Only for $s = 1/2$ is the $\chi(T)$ curve out of this bundle. Hence, one can argue that, for $s > 1/2$, quantum effects in χ are almost negligible at normalized temperatures $T/s(s+1) \gtrsim 0.4$. The situation is quite different for the

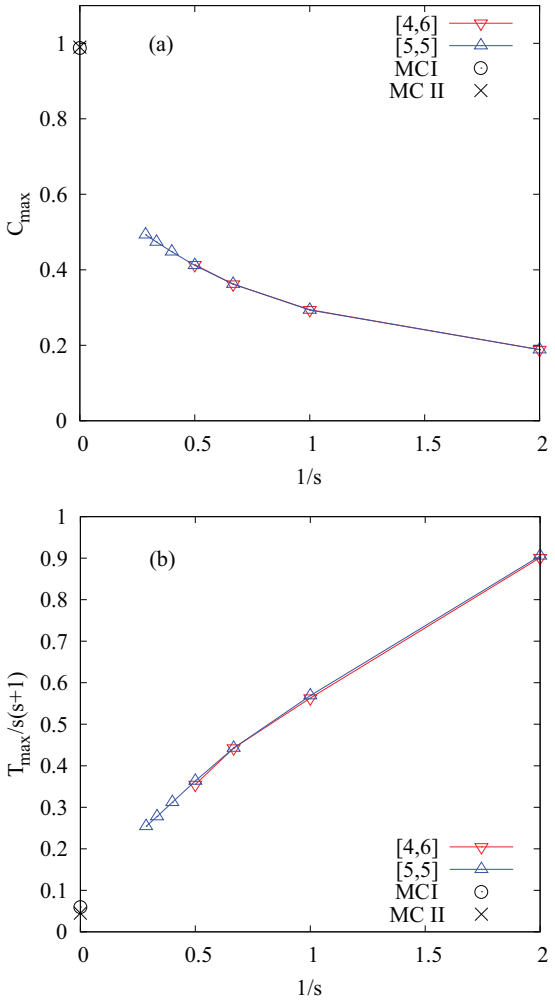

FIG. 7. (Color online) (a) Height C_{max} and (b) position T_{max} of the maximum in the specific heat C in dependence on the inverse spin quantum number $1/s$ of the kagome Heisenberg antiferromagnet. The Monte Carlo results for $s \to \infty$ are taken from Ref. 20 (MC I) and Ref. 21 (MC II). Note, however, that the maximum in $C(T)$ for the classical model is not well pronounced, rather there is a fairly broad region of high values of C.[21]

specific heat C, cf. Fig. 6. The maximum in $C(T)$, already mentioned above for $s = 1/2$, is evidently dependent on the spin quantum number s: Its position $T_{max}/s(s+1)$ is shifted to lower normalized temperatures, and its height C_{max} increases with growing s. Hence, the quantum effects seem to also be important for quite large values of s. The basic difference in the influence of s on $\chi(T)$ and $C(T)$ can be attributed to an exceptional density of low-lying singlet excitations, see, e.g., Ref. 6. These nonmagnetic excitations are irrelevant for χ but are important for C. Hence, our HTE-Padé data for $C(T)$ can also be understood as an indirect indication for the existence of an unusual large density of low-lying singlet excitation for $s > 1/2$. In Fig. 7, we show the position $T_{max}/s(s+1)$ and the height C_{max} as a function of $1/s$. From Fig. 6(a), it is obvious that, for the [4,6]-Padé approximant, a maximum exists only for $s < 5/2$. The tendency of how the classical limit is approached is clearly visible from our HTE data. There is, indeed, a remarkably strong dependence on the spin quantum number. The slope of the corresponding curves shown in Fig. 7 is even increasing when approaching the classical limit $1/s = 0$. Let us mention that, for the above discussion of the maximum of the specific heat, the eighth-order HTE presented in our previous paper[39] is not appropriate since the corresponding [4,4]-Padé approximant exhibits an unphysical pole in the vicinity of the maximum for $s > 1/2$.

IV. CONCLUSIONS

In this paper, we present the HTE series up to tenth order of the specific heat C and the uniform susceptibility χ for Heisenberg models with arbitrary exchange patterns $J_{\mu\nu}$ and spin quantum number s. Our HTE scheme is encoded in a C++ program using, as input, the exchange matrix $J_{\mu\nu}$ and spin quantum number s. Using Padé approximants for the HTE series, the scheme can be used to discuss thermodynamic properties of general Heisenberg systems down to moderate temperatures of about $T/s(s+1) \sim 0.4 \cdots 0.5$ and, thus, for the interpretation of experimental data in a rather wide temperature range, especially, if other precise methods, such as the quantum Monte Carlo method or the finite-temperature density matrix renormalization-group approach are not applicable. We apply our scheme to the 3D pyrochlore ferromagnet to calculate the Curie temperature T_c in dependence on the spin quantum number s. Comparing T_c of the pyrochlore ferromagnet with corresponding values for the simple-cubic ferromagnet, we find that the triangular configuration of bonds present in the pyrochlore lattices leads to a noticeable lowering of T_c. Using our HTE scheme for the kagome antiferromagnet, we discuss the influence of s on the temperature dependence of C and χ. Although the effect of s on χ in the accessible temperature range is rather weak, there is a well-pronounced shift in the maximum in the temperature dependence of specific heat to lower renormalized temperatures $T/s(s+1)$ when increasing s.

ACKNOWLEDGMENT

J.R. thanks A. Hauser and M. Maksymenko for fruitful discussions.

APPENDIX A : THE HIGH-TEMPERATURE EXPANSION FOR THE SUSCEPTIBILITY AND THE SPECIFIC HEAT FOR THE HEISENBERG MODEL ON THE PYROCHLORE LATTICE

The general formulas for the susceptibility and the specific heat for the Heisenberg model on the pyrochlore lattice with NN exchange constant J up to eighth order can be found in Ref. 39. For the sake of consistency with this reference, we have set $\beta = \frac{1}{k_B T}$ in Appendixes A and B, which is slightly different from the definition in Sec. II. The formulas for the

ninth and tenth orders read for the susceptibility,

$$\begin{aligned}
\chi(\beta) &= \frac{N}{J}\sum_{n=1}^{\infty} c_n (J\beta)^n, \\
c_9 &= \frac{1}{5143\,824\,000} r^2(-2710\,665 + 142\,840\,908r - 2195\,288\,001r^2 + 14\,497\,581\,366r^3 \\
&\quad - 45\,972\,407\,664r^4 + 77\,794\,619\,872r^5 - 82\,650\,432\,896r^6 + 46\,730\,617\,088r^7), \\
c_{10} &= -\frac{1}{169\,746\,192\,000} r^2(51\,519\,240 - 2994\,073\,848r + 51\,386\,055\,291r^2 \\
&\quad - 396\,940\,170\,060r^3 + 1579\,391\,570\,694r^4 - 3442\,568\,263\,344r^5 + 4692\,701\,814\,464r^6 \\
&\quad - 4374\,573\,206\,272r^7 + 2124\,654\,831\,616r^8).
\end{aligned} \tag{A1}$$

and for the specific heat,

$$\begin{aligned}
C(\beta) &= Nk\sum_{n=2}^{\infty} d_n (J\beta)^n, \\
d_9 &= -\frac{1}{285\,768\,000} r^2(-1807\,110 + 91\,861\,560r - 1255\,862\,151r^2 + 6268\,644\,864r^3 \\
&\quad - 8882\,615\,472r^4 - 1691\,186\,688r^5 - 21\,317\,760r^6 + 1042\,017\,280r^7), \\
d_{10} &= -\frac{1}{6286\,896\,000} r^2(-25\,759\,620 + 1451\,298\,330r - 22\,610\,800\,701r^2 \\
&\quad + 142\,189\,820\,847r^3 - 349\,296\,723\,134r^4 + 154\,955\,752\,848r^5 \\
&\quad + 102\,919\,717\,624r^6 + 82\,927\,576\,960r^7 - 11\,100\,907\,520r^8),
\end{aligned} \tag{A2}$$

where $r = s(s+1)$.

APPENDIX B : THE HIGH-TEMPERATURE EXPANSION FOR THE SUSCEPTIBILITY AND THE SPECIFIC HEAT FOR THE HEISENBERG MODEL ON THE KAGOME LATTICE

The general formulas for the Heisenberg model on the kagome lattice with NN exchange constant J read for the susceptibility,

$$\begin{aligned}
\chi(\beta) &= \frac{N}{J}\sum_{n=1}^{\infty} c_n (J\beta)^n, \\
c_1 &= \frac{1}{3} r, \\
c_2 &= -\frac{4}{9} r^2, \\
c_3 &= \frac{1}{9} r^2(-1+4r), \\
c_4 &= -\frac{4}{405} r^2(3 - 28r + 37r^2), \\
c_5 &= \frac{1}{4860} r^2(-45 + 702r - 1892r^2 + 1328r^3), \\
c_6 &= -\frac{1}{510\,300} r^2(1728 - 35\,946r + 164\,289r^2 - 207\,896r^3 + 102\,576r^4), \\
c_7 &= \frac{1}{6123\,600} r^2(-8694 + 218\,916r - 1401\,381r^2 + 2888\,772r^3 - 2251\,248r^4 + 909\,184r^5), \\
c_8 &= -\frac{1}{22\,963\,500} r^2(15\,390 - 446\,256r + 3538\,764r^2 - 10\,535\,337r^3 + 12\,202\,552r^4 - 7318\,640r^5 + 2416\,640r^6), \\
c_9 &= \frac{1}{7715\,736\,000} r^2(-2710\,665 + 87\,954\,822r - 807\,482\,331r^2 + 3091\,042\,674r^3 - 5118\,502\,560r^4 + 4009\,481\,184r^5 \\
&\quad - 2113\,197\,952r^6 + 518\,354\,176r^7),
\end{aligned} \tag{B1}$$

$$c_{10} = -\frac{1}{1273\,096\,440\,000} r^2 (257\,596\,200 - 9180\,862\,110r + 93\,799\,827\,171r^2 - 426\,255\,134\,022r^3 + 931\,126\,345\,494r^4 - 977\,085\,756\,168r^5 + 621\,427\,831\,616r^6 - 280\,517\,703\,040r^7 + 48\,779\,713\,280r^8),$$

and for the specific heat,

$$\begin{aligned}
C(\beta) &= Nk \sum_{n=2}^{\infty} d_n (J\beta)^n, \\
d_2 &= \frac{2}{3} r^2, \\
d_3 &= -\frac{1}{9} r^2 (-3 + 4r), \\
d_4 &= -\frac{2}{45} r^2 (-3 + 23r + 3r^2), \\
d_5 &= \frac{1}{162} r^2 (9 - 126r + 116r^2 + 48r^3), \\
d_6 &= -\frac{1}{68\,040} r^2 (-1728 + 33\,426r - 102\,969r^2 - 19\,464r^3 + 2144r^4), \\
d_7 &= -\frac{1}{97\,200} r^2 (-1242 + 29\,556r - 150\,039r^2 + 96\,676r^3 + 64\,544r^4 + 20\,992r^5), \\
d_8 &= \frac{1}{1093\,500} r^2 (7695 - 213\,084r + 1435\,806r^2 - 2537\,523r^3 - 539\,132r^4 + 58\,400r^5 + 186\,680r^6), \\
d_9 &= \frac{1}{214\,326\,000} r^2 (903\,555 - 28\,196\,370r + 227\,949\,579r^2 - 634\,514\,526r^3 + 285\,950\,568r^4 + 230\,120\,832r^5 \\
&\quad + 135\,526\,080r^6 + 14\,890\,240r^7), \\
d_{10} &= -\frac{1}{18\,860\,688\,000} r^2 (-51\,519\,240 + 1775\,187\,630r - 16\,326\,321\,219r^2 + 59\,250\,202\,038r^3 - 69\,170\,925\,596r^4 \\
&\quad - 15\,707\,506\,528r^5 - 728\,311\,984r^6 + 9196\,378\,240r^7 + 3884\,989\,440r^8).
\end{aligned} \tag{B2}$$

*johannes.richter@physik.uni-magdeburg.de

[1] C. Lhuillier and G. Misguich, in *High Magnetic Fields: Applications in Condensed Matter Physics and Spectroscopy*, edited by C. Berthier, L. P. Lévy, and G. Martinez, Lecture Notes in Physics Vol. 595 (Springer, Berlin, 2001), pp. 161–190; G. Misguich and C. Lhuillier, in *Frustrated Spin Systems*, edited by H. T. Diep (World Scientific, Singapore, 2005), pp. 229–306; J. Richter, J. Schulenburg, and A. Honecker, in *Quantum Magnetism*, edited by U. Schollwöck, J. Richter, D. J. J. Farnell, and R. F. Bishop, Lecture Notes in Physics Vol. 645 (Springer, Berlin, 2004), pp. 85–153; *Introduction to Frustrated Magnetism: Materials, Experiments, Theory*, edited by C. Lacroix, P. Mendels, and F. Mila (Springer, Berlin, 2011).

[2] M. Troyer and U.-J. Wiese, Phys. Rev. Lett. **94**, 170201 (2005).

[3] L. Balents, Nature (London) **464**, 199 (2010).

[4] C. Nisoli, R. Moessner, and P. Schiffer, Rev. Mod. Phys. **85**, 1473 (2013).

[5] P. W. Leung and V. Elser, Phys. Rev. B **47**, 5459 (1993).

[6] C. Waldtmann, H.-U. Everts, B. Bernu, C. Lhuillier, P. Sindzingre, P. Lecheminant, and L. Pierre, Eur. Phys. J. B **2**, 501 (1998).

[7] M. Mambrini and F. Mila, Eur. Phys. J. B **17**, 651 (2000).

[8] R. R. P. Singh and D. A. Huse, Phys. Rev. B **76**, 180407(R) (2007).

[9] P. Sindzingre and C. Lhuillier, Europhys. Lett. **88**, 27009 (2009).

[10] G. Evenbly and G. Vidal, Phys. Rev. Lett. **104**, 187203 (2010).

[11] S. Yan, D. A. Huse, and S. R. White, Science **332**, 1173 (2011).

[12] A. M. Läuchli, J. Sudan, and E. S. Sørensen, Phys. Rev. B **83**, 212401 (2011).

[13] H. Nakano and T. Sakai, J. Phys. Soc. Jpn. **80**, 053704 (2011).

[14] O. Götze, D. J. J. Farnell, R. F. Bishop, P. H. Y. Li, and J. Richter, Phys. Rev. B **84**, 224428 (2011).

[15] S. Depenbrock, I. P. McCulloch, and U. Schollwöck, Phys. Rev. Lett. **109**, 067201 (2012).

[16] Z. Y. Xie, J. Chen, J. F. Yu, X. Kong, B. Normand, and T. Xiang, arXiv:1307.5696.

[17] Y. Iqbal, D. Poilblanc, and F. Becca, arXiv:1311.5038.

[18] J. T. Chalker, P. C. W. Holdsworth, and E. F. Shender, Phys. Rev. Lett. **68**, 855 (1992).

[19] J. N. Reimers and A. J. Berlinsky, Phys. Rev. B **48**, 9539 (1993).

[20] A. J. Garcia-Adeva and D. L. Huber, Phys. Rev. B **63**, 140404 (2001).

[21] M. E. Zhitomirsky, Phys. Rev. B **78**, 094423 (2008).

[22] G.-W. Chern and R. Moessner, Phys. Rev. Lett. **110**, 077201 (2013).

[23]W. Opechowski, Physica **4**, 181 (1937).
[24]G. S. Rushbrooke and P. J. Wood, Proc. Phys. Soc., London, Sect. A **68**, 1161 (1955).
[25]P. J. Wood and G. S. Rushbrooke, Proc. Phys. Soc., London, Sect. A **70**, 765 (1957).
[26]G. S. Rushbrooke and P. J. Wood, Mol. Phys. **1**, 257 (1958).
[27]P. J. Wood and N. W. Dalton, Phys. Rev. **159**, 384 (1967).
[28]N. W. Dalton and D. E. Rimmer, Phys. Lett. **29A**, 611 (1969).
[29]G. S. Rushbrooke, G. A. Baker, Jr., and P. J. Wood, in *Phase Transitions and Critical Phenomena*, edited by C. Domb and M. S. Green (Academic, London, 1974), Vol. 3, p. 245.
[30]J. Oitmaa, C. J. Hamer, and W. H. Zheng, *Series Expansion Methods* (Cambridge University Press, Cambridge, UK, 2006).
[31]N. Elstner, R. R. P. Singh, and A. P. Young, Phys. Rev. Lett. **71**, 1629 (1993).
[32]N. Elstner and A. P. Young, Phys. Rev. B **50**, 6871 (1994).
[33]R. R. P. Singh and J. Oitmaa, Phys. Rev. B **85**, 104406 (2012).
[34]J. Reuther, P. Wölfle, R. Darradi, W. Brenig, M. Arlego, and J. Richter, Phys. Rev. B **83**, 064416 (2011).
[35]S. Nishimoto, S.-L. Drechsler, R. O. Kuzian, J. van den Brink, J. Richter, W. E. A. Lorenz, Y. Skourski, R. Klingeler, and B. Büchner, Phys. Rev. Lett. **107**, 097201 (2011).
[36]J. Oitmaa and E. Bornilla, Phys. Rev. B **53**, 14228 (1996).
[37]B. Bernu, C. Lhuillier, E. Kermarrec, F. Bert, P. Mendels, R. H. Colman, and A. S. Wills, Phys. Rev. B **87**, 155107 (2013).
[38]H.-J. Schmidt, J. Schnack, and M. Luban, Phys. Rev. B **64**, 224415 (2001).
[39]H.-J. Schmidt, A. Lohmann, and J. Richter, Phys. Rev. B **84**, 104443 (2011).
[40]URL: http://www.uni-magdeburg.de/jschulen/HTE/
[41]See Supplemental Material at http://link.aps.org/supplemental/10.1103/PhysRevB.89.014415 for five files: (i) manual.pdf, (ii) HTE10.tar.gz, (iii) Supplemental Material 1.nb, (iv) Supplemental Material 2.nb, and (v) Supplemental Material 3.nb. (i) contains a manual on how to use the code; (ii) contains the code itself; (iii)–(v) contain three MATHEMATICA 8.0.1 files containing the coefficients of the HTE of the moments, the specific heat, and the zero-field uniform susceptibility for general Heisenberg Hamiltonians up to tenth order.
[42]The C++ code can also be downloaded from http://www.uni-magdeburg.de/jschulen/HTE10/. We recommend using this URL, since available updates of the code (fixing of bugs, improvement of the code, etc.) will be provided there.
[43]G. A. Baker, Phys. Rev. **124**, 768 (1961).
[44]R. Moessner, Can. J. Phys. **79**, 1283 (2001).
[45]S. T. Bramwell and M. J. P. Gingras, Science **294**, 1495 (2001).
[46]C. Castelnovo, R. Moessner, and S. L. Sondhi, Nature (London) **451**, 42 (2008).
[47]J. M. Yeomans, *Statistical Mechanics of Phase Transitions* (Clarendon Press, Oxford, 1992).
[48]M. Troyer, F. Alet, and S. Wessel, Braz. J. Phys. **34**, 377 (2004); S. Wessel, Phys. Rev. B **81**, 052405 (2010).
[49]P. Peczak, A. M. Ferrenberg, and D. P. Landau, Phys. Rev. B **43**, 6087 (1991).
[50]Except for the analysis of $q_n = c_n/c_{n-1}$, other methods are known to analyze the series of c_n, see, e.g., Refs. 24 and 26. A more detailed analysis of those methods goes beyond the scope of the present paper.
[51]D. Schmalfuß, J. Richter, and D. Ihle, Phys. Rev. B **72**, 224405 (2005).
[52]A. B. Harris, C. Kallin, and A. J. Berlinsky, Phys. Rev. B **45**, 2899 (1992).
[53]S. Sachdev, Phys. Rev. B **45**, 12377 (1992).
[54]T. Nakamura and S. Miyashita, Phys. Rev. B **52**, 9174 (1995).
[55]P. Tomczak and J. Richter, Phys. Rev. B **54**, 9004 (1996).
[56]P. Sindzingre, G. Misguich, C. Lhuillier, B. Bernu, L. Pierre, C. Waldtmann, and H.-U. Everts, Phys. Rev. Lett. **84**, 2953 (2000).
[57]B. H. Bernhard, B. Canals, and C. Lacroix, Phys. Rev. B **66**, 104424 (2002).
[58]G. Misguich and B. Bernu, Phys. Rev. B **71**, 014417 (2005).
[59]M. Rigol, T. Bryant, and R. R. P. Singh, Phys. Rev. E **75**, 061118 (2007).
[60]G. Misguich and P. Sindzingre, Eur. Phys. J. B **59**, 305 (2007).
[61]A. S. Wills, A. Harrison, C. Ritter, and R. I. Smith, Phys. Rev. B **61**, 6156 (2000).
[62]B. Fak, F. C. Coomer, A. Harrison, D. Visser, and M. E. Zhitomirsky, Europhys. Lett. **81**, 17006 (2008).
[63]S.-H. Lee, C. Broholm, M. F. Collins, L. Heller, A. P. Ramirez, C. Kloc, E. Bucher, R. W. Erwin, and N. Lacevic, Phys. Rev. B **56**, 8091 (1997).
[64]Y. J. Uemura, A. Keren, K. Kojima, L. P. Le, G. M. Luke, W. D. Wu, Y. Ajiro, T. Asano, Y. Kuriyama, M. Mekata, H. Kikuchi, and K. Kakurai, Phys. Rev. Lett. **73**, 3306 (1994); B. Martínez, F. Sandiumenge, A. Rouco, A. Labarta, J. Rodríguez-Carvajal, M. Tovar, M. T. Causa, S. Gali, and X. Obradors, Phys. Rev. B **46**, 10786 (1992).
[65]D. E. Freedman, R. Chisnell, T. M. McQueen, Y. S. Lee, C. Payen, and D. G. Nocera, Chem. Commun. (Cambridge, UK) **48**, 64 (2012).
[66]In Ref. 32, there is a misprint in the seventh-order coefficient for χ. The coefficient 2711 184 given in Ref. 32 has to be replaced by 2711 296.